

# Stringy (holographic) Pomeron with extrinsic curvature

Yachao Qian and Ismail Zahed

*Department of Physics and Astronomy, Stony Brook University, Stony Brook, New York 11794-3800, USA*  
 (Received 7 March 2015; published 8 October 2015)

We model the soft Pomeron in QCD using a scalar Polyakov string with extrinsic curvature in the bottom-up approach of holographic QCD. The overall dipole-dipole scattering amplitude in the soft Pomeron kinematics is shown to be sensitive to the extrinsic curvature of the string for finite momentum transfer. The characteristics of the diffractive peak in the differential elastic  $pp$  scattering are affected by a small extrinsic curvature of the string.

DOI: 10.1103/PhysRevD.92.085012

PACS numbers: 12.38.-t

## I. INTRODUCTION

The high energy proton on proton (antiproton) cross sections are dominated by Pomeron exchange, an effective object corresponding to the highest Regge trajectory. The slowly rising cross sections are described by the soft Pomeron with intercept  $\alpha_p(0) - 1 \approx 0.08$  and vacuum quantum numbers. Reggeon exchanges have smaller intercepts and are therefore subleading. Reggeon theory for hadron-hadron scattering with large rapidity intervals provides an effective explanation for the transverse growth of the cross sections [1].

The transverse growth of the proton with rapidity  $\chi$  follows from the Balitsky-Fadin-Kuraev-Lipatov (BFKL) ladders [2–6] at weak coupling in QCD. Collinear gluon bremsstrahlung is large even when the coupling is weak and requires resummation. The ensuing BFKL hard Pomeron carries a large intercept and zero slope. The intercept is slightly improved by higher order perturbative corrections to the BFKL ladder.

The soft Pomeron kinematics suggests an altogether non-perturbative approach. Through duality arguments, Veneziano suggested long ago that the soft Pomeron is a closed string exchange [7]. In QCD the closed string world sheet can be thought of as the surface spanned by planar gluon diagrams or fishnets [8]. The quantum theory of planar diagrams in supersymmetric gauge theories is tractable in the double limit of a large number of colors  $N_c$  and 't Hooft coupling  $\lambda = g^2 N_c$  using the AdS/CFT holographic approach [9].

In the past decade there have been several attempts at describing the soft Pomeron using holographic QCD [10–32]. In this paper we follow the work in [23–26] and describe the soft Pomeron as an effective string with extrinsic curvature in 5 dimensions. This is inherently a bottom-up approach with the holographic or 5th direction playing the role of the scale dimension for the closed string. The geometry is that of AdS<sub>5</sub> with a wall. In the UV AdS<sub>5</sub> enforces conformality which is a property of QCD-BFKL kernels, while in the IR the wall enforces confinement as a generic feature of QCD.

In Sec. II, we review the setup for dipole-dipole scattering through a closed string exchange. In Sec. III,

we introduce the QCD effective action with a finite string tension and extrinsic curvature and use it to derive the closed string exchange propagator in flat  $5 = 2 + D_\perp$  dimensions. In Sec. IV, we detail how the extrinsic curvature modifies the correlation of twisted Wilson loops, and show how it affects the position of the diffractive peak in the differential elastic  $pp$  scattering cross section. Our conclusions are in Sec. V. In the Appendix, we show how the extrinsic curvature affects the stringy interaction between two static dipoles.

## II. DIPOLE-DIPOLE SCATTERING

In this section, we briefly review the setup for dipole-dipole scattering using an effective string theory. For that, we follow [23] and consider the elastic scattering of two dipoles,

$$D_1(p_1) + D_2(p_2) \rightarrow D_1(k_1) + D_2(k_2) \quad (2.1)$$

as depicted in Fig. 1.  $a_T$  and  $a_L$  are the dipoles' transverse and longitudinal lengths, respectively, set near the UV boundary of AdS<sub>5</sub>,  $b$  is an impact parameter and the angle  $\theta$  is the Euclidean analogue of the rapidity interval

$$\cosh \chi = \frac{s}{2m^2} - 1 \rightarrow \cos \theta \quad (2.2)$$

with  $s = (p_1 + p_2)^2$  [33,34]. Following the same argument as in [23], the scattering amplitude  $\mathcal{T}$  in Euclidean space is given by

$$\frac{1}{-2is} \mathcal{T}(\theta, q) \approx \int d^2 \mathbf{b} e^{i\mathbf{q}_\perp \cdot \mathbf{b}} \left\langle \mathbf{W} \left( -\frac{\theta}{2}, -\frac{b}{2} \right) \mathbf{W} \left( \frac{\theta}{2}, \frac{b}{2} \right) - 1 \right\rangle \quad (2.3)$$

where

$$\mathbf{W}(\theta, \mathbf{b}) = \frac{1}{N_c} \text{tr} \left[ \mathbf{P}_c \exp \left( ig \int_{c_o} d\tau \mathbf{A}(\mathbf{x}) \cdot \mathbf{v} \right) \right] \quad (2.4)$$

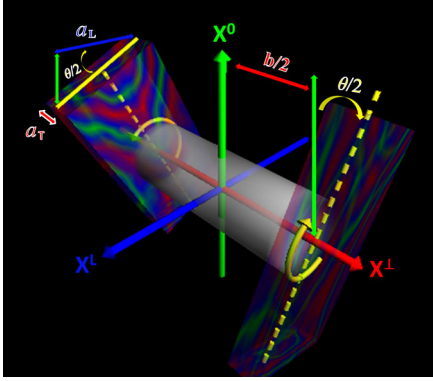


FIG. 1 (color online). Dipole-dipole scattering.

is the normalized Wilson loop for a dipole with  $\langle \mathbf{W} \rangle = 1$ .  $C_\theta$  is the closed rectangular loop in Fig. 1. For simplicity, we denote the Euclidean loop correlator as  $\mathbf{W}\mathbf{W}$ . Considering one closed string exchange between dipoles, we have

$$\begin{aligned} \langle \mathbf{W}\mathbf{W} \rangle &\equiv \left\langle \mathbf{W} \left( -\frac{\theta}{2}, -\frac{b}{2} \right) \mathbf{W} \left( \frac{\theta}{2}, \frac{b}{2} \right) - 1 \right\rangle \\ &= g_s^2 \int \frac{dT}{2T} \mathbf{K}(T) \end{aligned} \quad (2.5)$$

where

$$\mathbf{K}(T) = \int_T \mathfrak{D}[x] e^{-S[x] + \text{ghost}} \quad (2.6)$$

is the string partition function on the cylinder topology with modulus  $T$ . The overall factor of  $g_s^2$  in (2.5) is due to the relative genus in comparison to the unconnected Wilson loops. This analysis of the soft Pomeron is different from the (distorted) spin-2 graviton exchange in [15–18] as the graviton is massive in walled AdS<sub>5</sub>. Our approach is similar to the one followed in [23] with the difference that  $2 + D_\perp = 5$  and not 10 [24–26]. It is essentially an effective approach along the bottom-up scenario of AdS<sub>5</sub> with metric

$$ds^2 = \frac{R^2}{z^2} ((dx^0)^2 + (dx^1)^2 + (dx_\perp)^2 + (dz)^2) \quad (2.7)$$

and  $0 \leq z \leq z_0$ .  $R$  is the size of the AdS space for  $z_0 = \infty$ . Although the dual field theory corresponding to this truncated version of AdS<sub>5</sub> metric is not QCD, it does capture some key aspects, i.e., conformality in the UV and confinement in the IR. A similar argument was made in [35] in calculating the light-front wave functions from the AdS/CFT holographic correspondence.

### III. K WITH EXTRINSIC CURVATURE

At large impact parameters  $\mathbf{b}$  and for fixed dipole sizes  $a$  on the boundary, the exchanged string in Fig. 1 is long and lies mostly along the wall at  $z \approx z_0$  whereby the metric is nearly flat [11,12,23–28]. In [23–26], the authors used the scalar Polyakov string action and showed that such a single closed string exchange yields a Regge behavior of the elastic amplitude. Note that the results are in agreement with those developed originally in [11,12] after correcting a few mistakes as detailed in [23]. We now revisit the analysis in [23–26] by considering the corrections due to the extrinsic curvature of the effective string action as advocated also by Polyakov [36]. The purpose is to extend the regime of validity of the approach for intermediate values of  $\mathbf{b}$  or momentum transfer  $|t|$ .

#### A. Effective string action

There are many indications from lattice simulations that flux tubes in Yang-Mills theory can be described by an effective theory of strings of which the Nambu-Goto (NG) action is a good approximation in leading order [37]. Polyakov has suggested that the NG action must include an effective contribution that accounts for the extrinsic curvature of the world sheet at next order. The extrinsic curvature favors smooth string configurations and penalizes strings with high curvature. Specifically, the scalar action in Polyakov form with extrinsic curvature is [36,38]

$$\begin{aligned} S[x] &= \frac{\sigma_T}{2} \int_0^T d\tau \int_0^1 d\sigma (\dot{x}^\mu \dot{x}_\mu + x'^\mu x'_\mu) \\ &\quad + \frac{1}{2\kappa b^2} \int_0^T d\tau \int_0^1 d\sigma (\ddot{x}^\mu \ddot{x}_\mu + 2\dot{x}'^\mu \dot{x}'_\mu + x''^\mu x''_\mu). \end{aligned} \quad (3.1)$$

We have set the gauge on the world sheet to be  $h_b^a = \delta_b^a$  and used the nearly flat metric  $g^{\mu\nu}(z \approx z_0) = \delta^{\mu\nu} R^2/z_0^2$  at the bottom of AdS<sub>5</sub> (long strings). Here  $\dot{x} = \partial_\tau x$  and  $x' = \partial_\sigma x$ . The string tension is  $\sigma_T = 1/(2\pi\alpha')$  with  $\alpha' = z_0^2/\sqrt{\lambda}$ , and the effective and dimensionless extrinsic curvature is  $\kappa = e z_0^2/R^2$ .

#### B. Boundary conditions

For small dipole size and large impact parameter, the boundaries of the funnel of the exchanged string will be pinched and can be approximated as two straight lines,

$$\begin{aligned} \cos\left(\frac{\theta}{2}\right)x^1 + \sin\left(\frac{\theta}{2}\right)x^0 \Big|_{\sigma=0} &= 0 \\ \cos\left(\frac{\theta}{2}\right)x^1 - \sin\left(\frac{\theta}{2}\right)x^0 \Big|_{\sigma=1} &= 0 \end{aligned} \quad (3.2)$$

and  $x^\mu$  is periodic along the  $\tau$  direction,

$$x^\mu(\tau) = x^\mu(\tau + T). \quad (3.3)$$

The twisted boundary condition [Eq. (3.2)] can be simplified as follows:

$$\begin{pmatrix} x^0 \\ x^1 \end{pmatrix} = \begin{pmatrix} \cos \frac{\theta_\sigma}{2} & -\sin \frac{\theta_\sigma}{2} \\ \sin \frac{\theta_\sigma}{2} & \cos \frac{\theta_\sigma}{2} \end{pmatrix} \begin{pmatrix} y^0 \\ y^1 \end{pmatrix} \quad (3.4)$$

with  $\theta_\sigma = \theta(2\sigma - 1)$ . As a result (3.2) are now ordinary Dirichlet boundary conditions,

$$y^1|_{\sigma=0,1} = 0. \quad (3.5)$$

By taking  $\partial_\tau$  on both sides of Eq. (3.5) and recalling that the world-sheet energy-momentum tensor is null, i.e.  $T^{\alpha\beta} = \delta S / \delta g_{\alpha\beta} = 0$ , we have

$$\begin{aligned} \partial_\tau y^1|_{\sigma=0,1} &= 0 \\ \partial_\sigma y^0|_{\sigma=0,1} &= 0. \end{aligned} \quad (3.6)$$

### C. Closed string propagator $\mathbf{K}$

The natural mode decomposition for the string coordinates is given by

$$\begin{aligned} y^0(\tau, \sigma) &= \sum_{m=-\infty}^{\infty} \sum_{n=0}^{\infty} y_{m,n}^0 \exp\left(i2\pi m \frac{\tau}{T}\right) \cos(\pi n \sigma) \\ y^1(\tau, \sigma) &= \sum_{m=-\infty}^{\infty} \sum_{n=1}^{\infty} y_{m,n}^1 \exp\left(i2\pi m \frac{\tau}{T}\right) \sin(\pi n \sigma) \\ x^\perp(\tau, \sigma) &= y^\perp(\tau, \sigma) = \left(\sigma - \frac{1}{2}\right) b^\perp \\ &\quad + \sum_{m=-\infty}^{\infty} \sum_{n=1}^{\infty} y_{m,n}^\perp \exp\left(i2\pi m \frac{\tau}{T}\right) \sin(\pi n \sigma) \end{aligned} \quad (3.7)$$

with  $b^\perp = (0, 0, b, 0, 0)$  along one of the 2 spatial perpendicular directions. A rerun of the arguments presented in [23,27] yields the closed string propagator  $\mathbf{K}$  in (2.6) in the form

$$\mathbf{K} = \mathbf{K}_{0L} \times \mathbf{K}_{\theta L} \times \mathbf{K}_\perp \times \mathbf{K}_{\text{ghost}}. \quad (3.8)$$

$\mathbf{K}_{0L}$  and  $\mathbf{K}_{\theta L}$  are the longitudinal zero and nonzero mode contributions, respectively,  $\mathbf{K}_\perp$  is the transverse

contribution, and  $\mathbf{K}_{\text{ghost}}$  is the ghost contribution. Their explicit forms are

$$\mathbf{K}_{0L} = \left\{ \prod_{m=-\infty}^{\infty} \left[ \frac{\sigma_T T}{2\pi} \left( \theta^2 + \frac{4\pi^2 m^2}{T^2} \right) + \frac{T}{2\kappa b^2 \pi} \left( \theta^2 + \frac{4\pi^2 m^2}{T^2} \right)^2 \right] \right\}^{-\frac{D_\perp}{2}}, \quad (3.9)$$

$$\mathbf{K}_{\theta L} = \left\{ \prod_{n=1}^{\infty} \prod_{s=\pm} \prod_{m=-\infty}^{\infty} \left[ \frac{\sigma_T T}{4\pi} \left( \frac{4m^2 \pi^2}{T^2} + (n\pi + s\theta)^2 \right) + \frac{T}{4\kappa b^2 \pi} \left( \frac{4m^2 \pi^2}{T^2} + (n\pi + s\theta)^2 \right)^2 \right] \right\}^{-\frac{D_\perp}{2}}, \quad (3.10)$$

$$\mathbf{K}_\perp = \exp\left[-\frac{\sigma_T}{2} T b^2\right] \left\{ \prod_{n=1}^{\infty} \prod_{m=-\infty}^{\infty} \left[ \frac{\sigma_T T}{4\pi} \left( \frac{4\pi^2 m^2}{T^2} + n^2 \pi^2 \right) + \frac{T}{4\kappa b^2 \pi} \left( \frac{4\pi^2 m^2}{T^2} + n^2 \pi^2 \right)^2 \right] \right\}^{-\frac{D_\perp}{2}}, \quad (3.11)$$

$$\mathbf{K}_{\text{ghost}} = \prod_{n=1}^{\infty} \prod_{m=-\infty}^{\infty} \left[ \frac{\sigma_T T}{4\pi} \left( \frac{4m^2 \pi^2}{T^2} + n^2 \pi^2 \right) + \frac{T}{4\kappa b^2 \pi} \left( \frac{4m^2 \pi^2}{T^2} + n^2 \pi^2 \right)^2 \right], \quad (3.12)$$

which are seen to reduce to those in [23,27] for  $\kappa = \infty$ . The ghost contribution beyond the scalar Polyakov action and for finite extrinsic curvature is assumed so as to cancel the  $s = \pm 1$  spurious nonzero modes contribution from the longitudinal contribution for  $\theta = 0$ . This assumption, while proved for  $\kappa = \infty$ , is now assumed for finite  $\kappa$ .

The string of diverging products can be regularized by standard zeta function regularization,

$$\sinh(\pi x) = \pi x \prod_{m=1}^{\infty} \left( 1 + \frac{x^2}{m^2} \right) \quad (3.13)$$

in terms of which the string partition function (3.8) now reads

$$\begin{aligned} \mathbf{K}(T, \kappa) &= \frac{a^2}{\alpha'} e^{-\frac{\sigma_T T b^2}{2}} \frac{1}{2 \sinh\left(\frac{\theta T}{2}\right)} \left[ \prod_{n=1}^{\infty} \prod_{s=\pm} \frac{\sinh\left(\frac{n\pi T}{2}\right)}{\sinh\left(\frac{T(n\pi + s\theta)}{2}\right)} \right] \left[ \prod_{n=1}^{\infty} 2 \sinh\left(\frac{n\pi T}{2}\right) \right]^{-D_\perp} \\ &\quad \times \frac{1}{2 \sinh\left(\frac{T}{2} \sqrt{\theta^2 + \sigma_T \kappa b^2}\right)} \prod_{n=1}^{\infty} \prod_{s=\pm} \frac{1}{2 \sinh\left[\frac{T(n\pi + s\theta)}{2} \sqrt{1 + \frac{\sigma_T \kappa b^2}{(n\pi + s\theta)^2}}\right]} 2^{D_\perp} \left[ 2 \prod_{n=1}^{\infty} \sinh\left(\frac{n\pi T}{2} \sqrt{1 + \frac{\sigma_T \kappa b^2}{n^2 \pi^2}}\right) \right]^{-D_\perp + 2} \end{aligned} \quad (3.14)$$

with

$$a^2 \rightarrow a_T^2 + \frac{a_L^2}{\sin^2(\frac{\theta}{2})} \rightarrow a_T^2 \quad (3.15)$$

as the longitudinal dipole size  $a_L$  is suppressed at large  $\chi$  after analytical continuation. Note that for large transverse impact parameter  $b$ ,

$$\begin{aligned} & \prod_{n=1}^{\infty} \prod_{s=\pm} 2 \sinh \left( \frac{T(n\pi+s\theta)}{2} \sqrt{1 + \frac{\sigma_T \kappa b^2}{(n\pi+s\theta)^2}} \right) \\ & \approx \exp \left[ - \sum_{n=1}^{\infty} \sum_{s=\pm} \frac{Tb\sqrt{\kappa\sigma_T}}{2} \left( 1 + \frac{1}{2} \frac{(n\pi+s\theta)^2}{\sigma_T \kappa b^2} + \dots \right) \right] \\ & \approx \exp \left( -\zeta(0) Tb\sqrt{\kappa\sigma_T} \sqrt{1 + \frac{\theta^2}{\sigma_T \kappa b^2}} \right) \\ & = \exp \left( \frac{T}{2} \sqrt{\sigma_T \kappa b^2 + \theta^2} \right) \end{aligned} \quad (3.16)$$

and

$$\begin{aligned} & \prod_{n=1}^{\infty} 2 \sinh \left( \frac{n\pi T}{2} \sqrt{1 + \frac{\sigma_T \kappa b^2}{n^2 \pi^2}} \right) \\ & \approx \exp \left[ \sum_{n=1}^{\infty} \frac{Tb\sqrt{\kappa\sigma_T}}{2} \left( 1 + \frac{1}{2} \frac{n^2 \pi^2}{\sigma_T \kappa b^2} + \dots \right) \right] \\ & = \exp \left( -\frac{Tb\sqrt{\kappa\sigma_T}}{4} \right) \end{aligned} \quad (3.17)$$

where we used  $\zeta(-2n) = 0$  ( $n = 1, 2, 3, \dots$ ). Thus (3.14) simplifies to

$$\mathbf{K}(T, \kappa) \approx \mathbf{K}_F(T) \exp \left[ \frac{(D_{\perp} - 2)}{4} Tb\sqrt{\kappa\sigma_T} \right] \quad (3.18)$$

with  $\mathbf{K}_F(T)$  the closed string propagator without the extrinsic curvature  $\kappa$ ,

$$\begin{aligned} \mathbf{K}_F(T) &= \frac{a^2}{\alpha'} \frac{e^{-\frac{\sigma_T}{2} T b^2}}{2 \sinh(\frac{\theta T}{2})} \prod_{n=1}^{\infty} \prod_{s=\pm} \frac{\sinh(\frac{n\pi T}{2})}{\sinh[\frac{T(n\pi+s\theta)}{2}]} \\ & \times \left[ \prod_{n=1}^{\infty} 2 \sinh \left( \frac{n\pi T}{2} \right) \right]^{-D_{\perp}}. \end{aligned} \quad (3.19)$$

The resulting (3.18) is rather similar to the one derived in one loop in [38] for a large and static Wilson loop. We now detail its impact on the scattering of two twisted dipoles with the soft Pomeron kinematics.

## IV. SCATTERING AMPLITUDE WITH EXTRINSIC CURVATURE

### A. Dipole-dipole scattering

The result (3.18) may now be used to estimate the dipole-dipole scattering amplitude of Sec. II. Indeed, inserting (3.18) into (2.5), and then analytically continuing  $\theta \rightarrow -i\chi$ , yields for the twisted Wilson-loop correlator,

$$\begin{aligned} \mathbf{W}\mathbf{W} &= \frac{g_s^2 a^2}{4\alpha'} \sum_{k=1}^{\infty} \frac{(-1)^k}{k} e^{-k\frac{\sigma_T b^2}{\chi}} \eta^{-D_{\perp}} \left( \frac{ik\pi}{\chi} \right) \\ & \times \exp \left[ \frac{(D_{\perp} - 2)k\pi}{2\chi} b\sqrt{\kappa\sigma_T} \right] \end{aligned} \quad (4.1)$$

where  $\eta(\tau)$  is a Dedekind eta function and  $\eta(ix) = \eta(i/x)/\sqrt{x}$  [23,27],

$$\begin{aligned} \eta^{-D_{\perp}} \left( \frac{ik\pi}{\chi} \right) &= \left( \frac{k\pi}{\chi} \right)^{\frac{D_{\perp}}{2}} e^{\frac{\chi D_{\perp}}{12k}} \prod_{n=1}^{\infty} \left( 1 - \exp \left[ -\frac{2n\chi}{k} \right] \right)^{-D_{\perp}} \\ &= \left( \frac{k\pi}{\chi} \right)^{\frac{D_{\perp}}{2}} e^{\frac{\chi D_{\perp}}{12k}} \sum_{n=0}^{\infty} d(n) e^{-n\frac{2\chi}{k}}. \end{aligned} \quad (4.2)$$

In momentum space, the scattering amplitude is

$$\begin{aligned} & \frac{1}{-2is} \mathcal{T}_{DD}(\chi, q) \\ & \approx \int d^2 \mathbf{b} e^{i\mathbf{q}_{\perp} \cdot \mathbf{b}} \langle \mathbf{W}\mathbf{W} \rangle \\ & \approx \frac{\pi^2 g_s^2 a^2}{2} \sum_{n=0}^{\infty} \sum_{k=1}^{\infty} d(n) \frac{(-1)^k}{k} \left( \frac{k\pi}{\chi} \right)^{\frac{D_{\perp}-2}{2}} \\ & \times \exp \left( \chi \frac{D_{\perp}}{12k} - \chi \frac{2n}{k} - \chi \frac{\mathbf{q}_{\perp}^2}{4\sigma_T k\pi} + \sqrt{\kappa} \frac{D_{\perp} - 2}{4} \frac{|\mathbf{q}_{\perp}|}{\sqrt{\sigma_T}} \right) \end{aligned} \quad (4.3)$$

where we used  $\chi \approx \ln s$  for large  $s$ . Recall that the sum over  $k$  runs over the N-ality of the gauge group which is up to  $[N_c/2] = \infty$  in the AdS/CFT correspondence [27]. For QCD,  $N_c = 3$  and  $[3/2] = 1$  which means only the  $k = 1$  term contributes to the scattering of two dipoles in the fundamental representation of  $SU(N_c)$ . The effect of the extrinsic curvature is a momentum dependent contribution to the exponent that is large but subleading at large  $\chi$ .

### B. $pp$ scattering

For a fixed impact parameter,  $\langle \mathbf{W}\mathbf{W} \rangle$  is the elastic amplitude of a dipole of size  $a$  onto a fixed dipole  $a' = a$ , both of which are fixed in the UV or on the boundary. In general, the dipole size in a given hadron, say  $p$  or  $\bar{p}$ , is scale dependent and identified with the holographic direction, i.e.  $a \rightarrow z = z_0 e^{-u(z)}$  and  $a' \rightarrow z' = z_0 e^{-u'(z')}$  with  $0 < u, u' < \infty$  [25]. With this in mind, the elastic

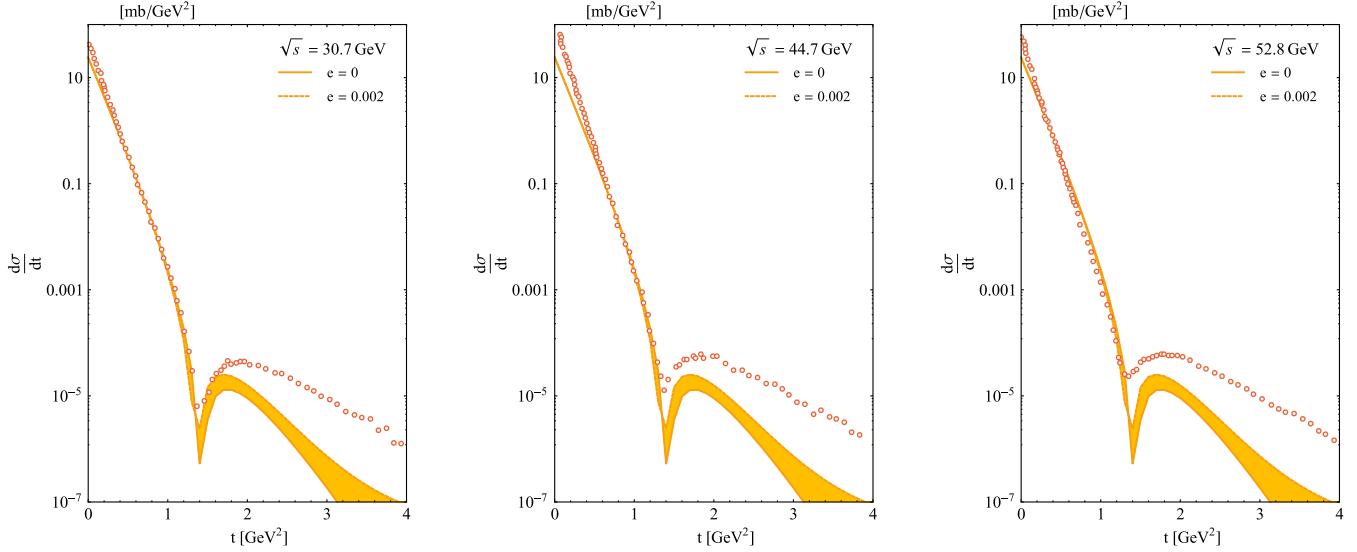


FIG. 2 (color online). Elastic differential  $pp$  cross section: solid curve stringy Pomeron with no extrinsic curvature  $\kappa = e = 0$ ; dashed curve with  $\kappa = e = 0.002$ . The data are from [40].

scattering amplitude for  $pp$  scattering  $p_1 p_2 \rightarrow p_1 p_2$  reads, in general,

$$\mathcal{T}_{pp}(\chi, \mathbf{b}) = \int_0^\infty du \int_0^\infty du' \psi_1^*(u) \psi_2^*(u') \times \mathcal{T}_{DD}(\chi, \mathbf{b}, u, u') \psi_1(u) \psi_2(u'). \quad (4.4)$$

In our case,  $|\psi_{1,2}(u, u')|^2 \equiv \mathcal{N}_p \delta(u, u' - u(a))$  for equal and fixed size dipoles  $a$ , and  $\mathcal{T}_{DD}$  is the dipole-dipole scattering amplitude. In the eikonal approximation, the elastic differential cross section reads

$$\frac{d\sigma}{dt} = \frac{1}{16\pi s^2} |\mathcal{T}_{pp}(\chi, q)|^2 = \frac{1}{4\pi} \left| i \int d\mathbf{b}^2 \int du \int du' e^{i\mathbf{q}_\perp \cdot \mathbf{b}} |\psi_1(u)|^2 |\psi_2(u')|^2 (1 - e^{\mathbf{W}\mathbf{W}}) \right|^2. \quad (4.5)$$

An optimal analysis of the available elastic differential  $pp$  data follows by setting  $D_\perp = 3$ ,  $N_c = 3$ ,  $\lambda = g^2 N_c = 9.4$ ,  $\kappa_g = 4\pi g_s/g^2 = 2.85$ ,  $z_0 = R = 0.4$  fm,  $\mathcal{N}_p = 1.5$ , and  $a = 0.25$  fm with a fixed rapidity interval  $\chi = 6$ . This parameter set is overall consistent with the one used in [25] for the analysis of the deep inelastic scattering data. The results are displayed in Fig. 2 and compared to the elastic  $pp$  data for  $\sqrt{s} = 30.7, 44.7, 52.8$  GeV from [39]. The solid curve is for no extrinsic curvature  $e = \kappa = 0$ , and the dashed curve is for  $e = \kappa = 0.002$ . The slope parameter  $\mathbf{B}(t)$  for the elastic differential cross section

$$\mathbf{B}(t) = \frac{d}{dt} \left( \ln \left( \frac{d\sigma}{dt} \right) \right) \quad (4.6)$$

is tabulated in Table I. While  $\mathbf{B}(t)$  does not change with a small change in the extrinsic curvature  $e$ , Fig. 2 shows that the depth and somehow the position of the diffractive peak are affected by a small extrinsic curvature for a stringy description of the Pomeron. The shaded region illustrates a

possible range of extrinsic curvatures that are compatible with the measured diffractive peak.

While a more exhaustive analysis of the parameter space, together with a better description of the dipole-dipole scattering amplitude at larger  $|t|$ , is needed, our estimates show an interesting interplay between the characteristics of the diffractive peak and the extrinsic curvature of the stringy Pomeron. Is this expected within the range of our analysis? To answer this question, we recall that in dipole-dipole scattering the use of the leading scalar Polyakov

TABLE I. Slope parameter  $\mathbf{B}(t)$  for the elastic differential cross section.

$\sqrt{s}$ [GeV]	$t$ [GeV <sup>2</sup> ]	$\mathbf{B}(t)$ [GeV <sup>-2</sup> ]		
		Experimental Data [39]	$e = 0$	$e = 0.002$
30.7	0.015–0.055	$13.0 \pm 0.7$	8.4	8.5
44.7	0.03–0.15	$12.9 \pm 0.4$	8.4	8.5
52.8	0.04–0.16	$13.0 \pm 0.3$	8.5	8.5

action [first term in (3.1)] is justified for large impact parameters  $\mathbf{b}$ , when the induced Unruh temperature  $1/\beta = 2\pi\mathbf{b}/\chi$  on the string world sheet is small in comparison to the Hagedorn temperature  $1/\beta_H = \sqrt{6/(D_\perp\alpha')}/2\pi$  [27,28,41,42],

$$\frac{\beta}{\beta_H} \equiv \frac{2\pi\mathbf{b}}{\chi\beta_H} > \frac{1}{\sqrt{2}} \quad (4.7)$$

with the string length  $\sqrt{\alpha'} = l_s \approx 0.1$  fm. For the above choice of parameters, this implies that  $\mathbf{b} > 4l_s/\sqrt{2} \approx 0.28$  fm, which puts the validity range at  $\sqrt{-t} \approx 1/\mathbf{b} \approx 0.7$  GeV. The inclusion of the extrinsic curvature [second term in (3.1)] extends the validity range to smaller  $\mathbf{b}$  or larger  $\sqrt{-t}$ . Our numerical analysis shows that these corrections are small with the exception of the region near the diffractive peak or  $\sqrt{-t} \approx 1$  GeV. Clearly, next to next to leading corrections in the string effective action as discussed in [43] may be needed to firm up the validity of this observation. Their analysis goes beyond the scope of this work. Finally, we note that if we were to relax the flat space approximation, the validity range can somehow be increased, as the effects of curvature on the stringy part of the dipole-dipole scattering can be schematically captured through an effective reduction in the transverse dimension  $D_\perp = 3 \rightarrow D_\perp(\lambda) < 3$  [24–26,28,29,41]. Thus, there is an effective increase in the Hagedorn temperature and a slightly lower bound on  $\mathbf{b}$  through (4.7).

## V. CONCLUSION

In holographic QCD, the Pomeron exchange in dipole-dipole scattering with a large rapidity  $\chi$  is described by the exchange of a noncritical string in hyperbolic  $D = 5$  dimensions. The extra (curved) direction is identified with the string scale dimension. In leading order, the Pomeron intercept is set by the Luscher-like term or  $D_\perp/12$  [23], and its slope is set by the string tension at the confinement scale. The curvature of the extra dimension causes the Pomeron intercept to shift from the Luscher term to order  $1/\sqrt{\lambda}$  [24–26].

Long color flux tubes in QCD are smooth. In leading order, the Nambu-Goto effective theory is corrected by a term that depends on the extrinsic curvature to allow for smooth string configurations [36]. The extrinsic curvature affects the zero point energy of large Wilson loops to one loop [38] and is amenable to lattice simulations. We have shown that a similar contribution affects the scattering amplitude of two dipoles. While there are higher order (loop) corrections to (4.3), the retained contributions are leading in the Pomeron kinematics.

In leading order, the extrinsic curvature induces an overall momentum dependent contribution to the scattering amplitude. A detailed comparison with accurate but differential proton on proton measurements at large  $\sqrt{s}$  but fixed

$t = -\mathbf{q}_\perp^2$  shows sensitivity of the diffractive peak to changes in the extrinsic curvature.  $pp$  scattering may provide for an empirical estimate of the extrinsic curvatures of smooth QCD strings, in addition to the current measurement estimates for the slope (string tension) and intercept (Luscher contribution) of the Pomeron.

## ACKNOWLEDGMENTS

This work was supported by the U.S. Department of Energy under Contract No. DE-FG-88ER40388.

## APPENDIX: STATIC AND STRINGY DIPOLE-DIPOLE INTERACTION

In this appendix, we detail the role of the extrinsic curvature on the correlator of two static but untwisted Wilson loops with  $\theta = 0$ , i.e. the interaction between two static dipoles. Instead of (3.7), we now have the mode decomposition

$$\begin{aligned} x^0(\tau, \sigma) &= \sum_{m=-\infty}^{\infty} \sum_{n=1}^{\infty} x_{m,n}^0 \exp\left(i2\pi m \frac{\tau}{T}\right) \cos(\pi n \sigma) + X + \frac{P}{\sigma_T} \tau \\ x^1(\tau, \sigma) &= \sum_{m=-\infty}^{\infty} \sum_{n=1}^{\infty} x_{m,n}^1 \exp\left(i2\pi m \frac{\tau}{T}\right) \sin(\pi n \sigma) \\ x^\perp(\tau, \sigma) &= \left(\sigma - \frac{1}{2}\right) b^\perp \\ &\quad + \sum_{m=-\infty}^{\infty} \sum_{n=1}^{\infty} x_{m,n}^\perp \exp\left(i2\pi m \frac{\tau}{T}\right) \sin(\pi n \sigma) \end{aligned} \quad (A1)$$

with  $P$  the number of windings in the temporal direction. The exchanged closed string is assumed to be infinitely thin in this case in the absence of the boosting kinematics for the two scattering dipoles in the text. This approximation is justified in the final result (A7)–(A9) below. With this in mind, a repeat of the algebra in Sec. III yields the string partition function

$$\mathbf{K}(T, \kappa) = \mathbf{K}_F(T) \exp\left(\frac{D_\perp}{4} T b \sqrt{\kappa \sigma_T}\right) \quad (A2)$$

with  $\mathbf{K}_F(T)$  the string propagator without the extrinsic curvature in (3.1),

$$\mathbf{K}_F(T) = \frac{a^2}{\alpha'} \exp\left(-\frac{\sigma_T}{2} T b^2 - \frac{TP^2}{2\sigma_T}\right) \left[\prod_{n=1}^{\infty} 2 \sinh\left(\frac{n\pi T}{2}\right)\right]^{-D_\perp}. \quad (A3)$$

In comparing to the result in [38], we note the occurrence of the same zero point energy (one loop)

$$E_0^{\text{non}} = -\frac{D_\perp}{4} \sqrt{\sigma_T \kappa}. \quad (A4)$$

This is to be compared with our result (3.18) for the twisted dipoles, and it shows the commonality between the untwisted and large Wilson loops and the twisted and far Wilson loops.

Now, we also notice that in our case,

$$x^0(\tau + T, \sigma) = x^0(\tau, \sigma) + \frac{P}{\sigma_T} T. \quad (\text{A5})$$

Thus,  $P = cW$  with  $W = 0, \pm 1, \pm 2, \dots$  with  $W$  the winding number and  $c$  a constant to be interpreted below. The propagators with different windings can be resummed using the Poisson summation formula

$$\begin{aligned} \sum_{W=-\infty}^{\infty} \mathbf{K}(T, \kappa) &= \sum_{W=-\infty}^{\infty} \frac{a^2}{\alpha'} \exp\left(-\frac{\sigma_T}{2} T b^2 - W^2 \frac{T c^2}{2\sigma_T} + \frac{D_{\perp}}{4} T b \sqrt{\kappa \sigma_T}\right) \left[ \prod_{n=1}^{\infty} 2 \sinh\left(\frac{n\pi T}{2}\right) \right]^{-D_{\perp}} \\ &= \sqrt{\frac{2\pi\sigma_T}{T c^2}} \frac{a^2}{\alpha'} \sum_{k=-\infty}^{\infty} \exp\left[-\frac{\sigma_T}{2} T b^2 \left(1 - \frac{D_{\perp} \sqrt{\kappa}}{2b\sqrt{\sigma_T}}\right) - k^2 \frac{2\pi^2 \sigma_T}{T c^2}\right] \eta^{-D_{\perp}}\left(i \frac{T}{2}\right) \end{aligned} \quad (\text{A6})$$

where  $\eta(\tau)$  is a Dedekind eta function and  $\eta(ix) = \eta(i/x)/\sqrt{x}$  [23,27]. Inserting (A6) into (2.5) yields

$$\begin{aligned} \mathbf{WW} &= \frac{g_s^2 a^2 \sqrt{\pi\sigma_T}}{4\alpha' |c|} \sum_{k=-\infty}^{\infty} \sum_{n=0}^{\infty} d(n) \int_0^{\infty} dT \left(\frac{T}{2}\right)^{\frac{D_{\perp}-3}{2}} \exp\left[-\frac{T}{2} \sigma_T b^2 \left(1 - \frac{D_{\perp} \sqrt{\kappa}}{2b\sqrt{\sigma_T}}\right) - \frac{2}{T} k^2 \frac{\pi^2 \sigma_T}{c^2} \left(1 + \frac{2n\pi c^2}{k^2 \pi^2 \sigma_T} - \frac{D_{\perp} c^2}{12k^2 \pi \sigma_T}\right)\right] \\ &= \frac{g_s^2 a^2 \sqrt{\sigma_T}}{\alpha'} \left(\frac{\pi}{|c|}\right)^{\frac{D_{\perp}}{2}} \sum_{k=-\infty}^{\infty} \sum_{n=0}^{\infty} d(n) \left(\frac{1 + \frac{2n\pi c^2}{k^2 \pi^2 \sigma_T} - \frac{D_{\perp} c^2}{12k^2 \pi \sigma_T}}{1 - \frac{D_{\perp} \sqrt{\kappa}}{2b\sqrt{\sigma_T}}}\right)^{\frac{D_{\perp}-1}{4}} \left(\frac{k}{b}\right)^{\frac{D_{\perp}-1}{2}} \\ &\quad \times \mathbf{K}_{\frac{D_{\perp}-1}{2}}\left(\frac{2bk\pi\sigma_T}{|c|} \sqrt{\left(1 - \frac{D_{\perp} \sqrt{\kappa}}{2b\sqrt{\sigma_T}}\right) \left(1 + \frac{2n\pi c^2}{k^2 \pi^2 \sigma_T} - \frac{D_{\perp} c^2}{12k^2 \pi \sigma_T}\right)}\right) \end{aligned} \quad (\text{A7})$$

which is the correlator between two static dipoles at large distances  $b \gg D_{\perp} \sqrt{\kappa/4\sigma_T}$ . The summation over  $k$  should be limited to  $k = [N_c/2] = 1$  for dipoles in the fundamental representation of  $SU(N_c)$  [27].  $d(n)$  is the canonical string density of states with  $d(0) = 1$ . The static dipole-dipole potential following from the smooth string exchange amounts to a tower of scalar exchanges with masses ( $k = 1$ )

$$m_n(b, c) = \frac{2\pi\sigma_T}{|c|} \sqrt{\left(1 - \frac{D_{\perp} \sqrt{\kappa}}{2b\sqrt{\sigma_T}}\right) \left(1 + \frac{2n\pi c^2}{\pi^2 \sigma_T} - \frac{D_{\perp} c^2}{12\pi \sigma_T}\right)} \quad (\text{A8})$$

at large distances  $b \gg D_{\perp} \sqrt{\kappa/4\sigma_T}$ . Without the extrinsic curvature and setting  $|c| \equiv 2\pi/\beta$ ,  $m_n$  is the mass spectrum for closed strings of (arbitrary) size  $\beta > \beta_H$ ,

$$m_n(\infty, 2\pi/\beta) = \sigma_T \beta \sqrt{1 - \frac{\beta_H^2}{\beta^2} + \frac{8\pi n}{\sigma_T \beta^2}}, \quad (\text{A9})$$

with the Hagedorn temperature  $\beta_H = \sqrt{\pi D_{\perp}/3\sigma_T}$ . Here  $1/\beta = |c|/2\pi$  plays the role of an effective temperature associated with the exchange of a closed (periodic) string.

- [1] L. Gribov, E. Levin, and M. Ryskin, *Phys. Rep.* **100**, 1 (1983).  
 [2] E. A. Kuraev, L. N. Lipatov, and V. S. Fadin, *Sov. Phys. JETP* **44**, 443 (1976).  
 [3] L. Lipatov, *Sov. J. Nucl. Phys.* **23**, 338 (1976).  
 [4] G. F. Sterman, [arXiv:hep-ph/9905548](https://arxiv.org/abs/hep-ph/9905548).

- [5] V. S. Fadin, E. Kuraev, and L. Lipatov, *Phys. Lett.* **60B**, 50 (1975).  
 [6] I. Balitsky and L. Lipatov, *Sov. J. Nucl. Phys.* **28**, 822 (1978).  
 [7] G. Veneziano, *Nuovo Cimento A* **57**, 190 (1968).  
 [8] J. Greensite, *Nucl. Phys.* **B249**, 263 (1985).

- [9] J. M. Maldacena, *Phys. Rev. Lett.* **80**, 4859 (1998).
- [10] M. Rho, S.-J. Sin, and I. Zahed, *Phys. Lett. B* **466**, 199 (1999).
- [11] R. Janik and R. B. Peshchanski, *Nucl. Phys.* **B586**, 163 (2000).
- [12] R. A. Janik, *Phys. Lett. B* **500**, 118 (2001).
- [13] J. Polchinski and M. J. Strassler, *Phys. Rev. Lett.* **88**, 031601 (2002).
- [14] J. Polchinski and M. J. Strassler, *J. High Energy Phys.* **05** (2003) 012.
- [15] R. C. Brower, J. Polchinski, M. J. Strassler, and C.-I. Tan, *J. High Energy Phys.* **12** (2007) 005.
- [16] R. C. Brower, M. J. Strassler, and C.-I. Tan, *J. High Energy Phys.* **03** (2009) 092.
- [17] R. C. Brower, M. Djuric, I. Sarcevic, and C.-I. Tan, *J. High Energy Phys.* **11** (2010) 051.
- [18] R. C. Brower, M. Djuric, I. Sarcevic, and C.-I. Tan, [arXiv:1106.5681](https://arxiv.org/abs/1106.5681).
- [19] Y. Hatta, E. Iancu, and A. Mueller, *J. High Energy Phys.* **01** (2008) 063.
- [20] Y. Hatta, E. Iancu, and A. Mueller, *J. High Energy Phys.* **01** (2008) 026.
- [21] J. L. Albacete, Y. V. Kovchegov, and A. Taliotis, *J. High Energy Phys.* **07** (2008) 074.
- [22] J. L. Albacete, Y. V. Kovchegov, and A. Taliotis, *AIP Conf. Proc.* **1105**, 356 (2009).
- [23] G. Basar, D. E. Kharzeev, H.-U. Yee, and I. Zahed, *Phys. Rev. D* **85**, 105005 (2012).
- [24] A. Stoffers and I. Zahed, *Phys. Rev. D* **87**, 075023 (2013).
- [25] A. Stoffers and I. Zahed, [arXiv:1210.3724](https://arxiv.org/abs/1210.3724).
- [26] A. Stoffers and I. Zahed, *Acta Phys. Pol. B Proc. Suppl.* **6**, 7 (2013).
- [27] Y. Qian and I. Zahed, [arXiv:1211.6421](https://arxiv.org/abs/1211.6421).
- [28] E. Shuryak and I. Zahed, *Phys. Rev. D* **89**, 094001 (2014).
- [29] Y. Qian and I. Zahed, *Phys. Rev. D* **91**, 125032 (2015).
- [30] L. Cornalba, M. S. Costa, and J. Penedones, *Phys. Rev. Lett.* **105**, 072003 (2010).
- [31] L. Cornalba, M. S. Costa, and J. Penedones, *J. High Energy Phys.* **03** (2010) 133.
- [32] L. Cornalba and M. S. Costa, *Phys. Rev. D* **78**, 096010 (2008).
- [33] E. V. Shuryak and I. Zahed, *Phys. Rev. D* **62**, 085014 (2000).
- [34] E. Meggiolaro, *Eur. Phys. J. C* **4**, 101 (1998).
- [35] S. J. Brodsky, G. F. de Tramond, and H. G. Dosch, *Nuovo Cimento Soc. Ital. Fis.* **036**, 265 (2013).
- [36] A. M. Polyakov, *Nucl. Phys.* **B268**, 406 (1986).
- [37] J. Kuti, *Proc. Sci.*, LAT2005 (2006) 001 [[arXiv:hep-lat/0511023](https://arxiv.org/abs/hep-lat/0511023)].
- [38] Y. Hidaka and R. D. Pisarski, *Phys. Rev. D* **80**, 074504 (2009).
- [39] U. Amaldi, R. Biancastelli, C. Bosio, G. Matthiae, J. Allaby *et al.*, *Phys. Lett.* **36B**, 504 (1971).
- [40] U. Amaldi and K. R. Schubert, *Nucl. Phys.* **B166**, 301 (1980).
- [41] Y. Qian and I. Zahed, [arXiv:1508.03760](https://arxiv.org/abs/1508.03760).
- [42] E. Shuryak and I. Zahed, *Phys. Rev. C* **88**, 044915 (2013).
- [43] O. Aharony and Z. Komargodski, *J. High Energy Phys.* **05** (2013) 118.